Stem cell factor is implicated in microenvironmental interactions and cellular dynamics of chronic lymphocytic leukemia

George I. Gavriilidis,[1*] Stavroula Ntoufa,[2*] Nikos Papakostantinou,[2] Konstantia Kotta,[2] Triantafyllia Koletsa,[3] Elisavet Chartomatsidou,[2] Theodoros Moysiadis,[2,4] Niki Stavroyianni,[5] Achilles Anagnostopoulos,[5] Eleni Papadaki,[6] Asterios S. Tsiftsoglou[1] and Kostas Stamatopoulos[2,4]

[1]Laboratory of Pharmacology, School of Pharmacy, Aristotle University of Thessaloniki, Thessaloniki, Greece; [2]Institute of Applied Biosciences, Centre for Research and Technology Hellas, Thessaloniki, Greece; [3]Department of Pathology, Faculty of Medicine, Aristotle University, Thessaloniki, Greece; [4]Department of Molecular Medicine and Surgery, Karolinska Institute, Stockholm, Sweden; [5]Hematology Department and HCT Unit, G. Papanicolaou Hospital, Thessaloniki, Greece and [6]Department of Medicine, University of Crete, Heraklion, Greece

[*]*GIG and SN contributed equally as co-first authors.*

 doi:10.3324/haematol.2019.236513

Received: August 29, 2019.

Accepted: March 24, 2020.

Pre-published: March 26, 2020.

Correspondence: *KOSTAS STAMATOPOULOS* - kostas.stamatopoulos@certh.gr

SUPPLEMENTARY METHODS

B cell enrichment

$CD19^+$ B cells were negatively selected from whole blood or tonsils using the RosetteSep B-cell enrichment kit (StemCell Technologies, Vancouver, BC, Canada) as previously described.[1] The purity of all preparations was checked by flow cytometry and always exceeded 95% for $CD19^+$ cells.

Quantification of SCF and c-kit mRNA expression

Quantification of *KITLG* and *KIT* mRNA levels was achieved by RQ-PCR (ThermoFisher Scientific) using specific primers (Kicqstart™ Primers, Sigma-Aldrich) for each splice variant. Briefly, one microgram of RNA was reversed transcribed to cDNA and a 3:50 aliquot of the RT product was used as the template for RQ-PCR. The β_2 microglobulin (B2M) gene was used as reference gene.[2] For RQ-PCR experiments all samples were run in duplicate. Data was analyzed using the 2-ΔΔCt algorithm.[3]

Western blotting for the detection of SCF and HIF-1α protein expression

Total cellular protein was isolated from purified B cells. Cells were washed twice with ice-cold phosphate-buffered saline and lysed with Pierce® RIPA Lysis and Extraction Buffer (ThermoFisher Scientific). Protein lysates were quantified using Pierce™ BCA Protein Assay Kit (ThermoFisher Scientific). 15 micrograms of protein were run on a 10% acrylamide SDS-PAGE gel under denaturing and reducing conditions and then transferred to PVDF membranes. Immunoblot analysis was performed using (a) rabbit anti-SCF monoclonal antibody which recognizes both SCF isoforms (KL-1/KL-2), (b) anti-SCF polyclonal antibody which recognizes the KL-1 isoform (Abcam), (c) goat anti-rabbit IgG H&L (HRP) antibody (Abcam), (d) anti-hypoxia inducible factor 1a (HIF-1α) mouse monoclonal antibody and (e) goat anti-mouse IgG H&L (HRP) antibody (R&D Systems) (**Supplemental Table 3**). To ensure equal loading, membranes were stripped and reprobed with monoclonal anti-β -actin–peroxidase antibody (Merck) and MagicMark™ XP (ThermoFisher Scientific) as a protein standard for molecular weight estimation. Chemiluminescent detection of the proteins of interest was performed with Luminata™ Classico Western HRP Substrate (Merck) and visualized with GeneGnome (Syngene) imaging system. Ratios of SCF protein band intensity relative to β-actin band intensity were calculated for each sample using the ImageJ software (http://rsbweb.nih.gov/ij/).

Cell culture conditions

Primary CLL cells and the HS-5 human bone marrow stromal cells cell line (ATCC® CRL-11882™) were cultured at 37^0C in 5% CO_2 atmosphere in RPMI 1640 supplemented with GlutaMAX™ Supplement (ThermoFisher Scientific) and 10% heat-inactivated fetal bovine serum (FBS) and 50μg/mL penicillin/streptomycin. For the short term co-cultures, HS-5 cells were seeded at a concentration of $5x10^4$/ml/well in a 24-well plate. 48 hours later, the confluence of the mesenchymal feeder layer was assessed by phase contrast microscopy and provided that it exceeded ~80%, $3x10^6$ primary CLL cells were then added (ratio of 60:1 based on initial HS-5 seeding). For the long term co-cultures, HS-5 cells were seeded at a concentration of $5x10^4$/ml/well in a 24-well plate and 15 hours later $3x10^6$ CLL cells were added. Cells were harvested at the indicated time points (24 hours or 72 hours from the addition of CLL cells) with mild trypsinization (ThermoFisher Scientific). Single cultures of primary CLL cells at a concentration of $3x10^6$ cells/ml were set-up as untreated controls.

Stimulation of the primary CLL cells was performed with goat F(ab)2 anti-human IgM or IgG Abs (10 or 20 ug/ml respectively for 3-6-24 hours; ThermoFisher Scientific) for the BcR; CpG ODN (2.5 ug/ml for 24-72 hours; ODN2006, Invivogen) for TLR9; and, CD40L/Enhancer (0.1/1 ug/ml for 24-72 hours; ALX-850-064-KI01, Enzo Life Sciences) for CD40. For oxidation experiments, primary CLL cells were incubated with 10 mM H_2O_2 for 24 hours.

Flow cytometry studies

Flow cytometry was used for the assessment of cell viability, apoptosis, mitochondrial mass, membrane potential and intracellular expression of SCF, HIF-1α and Ki-67. All primary cell samples were stained for surface CD19 (PE-Cy™5 mouse anti-human CD19 antibody, BD) and viability (Fixable Viability Stain 660/FVS660; BD) prior to intracellular staining of SCF and Ki-67 (rabbit anti-SCF monoclonal antibody, monoclonal rabbit IgG, as isotypic control and goat anti-rabbit IgG H&L PE-labeled antibody (Abcam) or FITC-labeled antibody (ThermoFischer Scientific) and anti-Ki-67 Set (BD). Intracellular staining of HIF-1α was performed with monoclonal mouse anti-HIF-1α antibody (R&D Systems) and anti-mouse IgG H&L FITC-labeled antibody (ThermoFischer Scientific) (**Supplemental Table 3**).

Intracellular staining was achieved with the Fixation/Permeabilization Solution Kit (Beckton Dickinson) following the manufacturer's instructions. Apoptotic primary CLL cells were determined using the Annexin V – FITC Assay kit (Exbio).

The determination of mitochondrial mass in primary CLL cells was performed using MitoTracker™ Green FM (ThermoFisher Scientific). The determination of mitochondrial

membrane potential in primary CLL cells was performed using MitoTracker™ Red CMXRos (ThermoFisher Scientific).

In all measurements, 10,000 events were acquired on a BD FACS Calibur flow cytometer. Analysis of raw data followed using the FlowJo software (BD). The gating strategy for all analyses included the exclusion of dead cells on a SSC/FVS plot and detection of $CD19^+$ cells on a SSC/CD19-PE-Cy5.5 plot.

Immunohistochemistry studies-details for samples

From the archives of the Pathology Department, Aristotle University of Thessaloniki, we randomly selected six cases of bone marrow biopsies and seven cases of lymph nodes, previously diagnosed with CLL infiltration, according to World Health Organization Classification of Tumors of the Hematopoietic and Lymphoid Tissues. All cases represented de novo CLL diagnoses. In two cases, concurrent bone marrow and lymph node biopsies were available. In addition, three cases of lymph nodes with histological findings of reactive lymphadenitis and one case of bone marrow biopsy with non-specific, reactive features were included in the study. All specimens were fixed in 10% neutral-buffered formalin. Bone marrow biopsies were decalcified in an EDTA-based solution.

Survival analysis

Firstly, time-dependent Receiver Operating Characteristic (ROC) curve analysis was used to assess the diagnostic accuracy of the SCF, measured at baseline (date of diagnosis) on overall survival (OS) and time-to-first-treatment (TTFT).[4] To detect the most appropriate threshold within SCF, and to accommodate the time effect at the same time, different time points from date of diagnosis were evaluated. In particular the time points 50, 100, 150, 200 and 258 months were considered, and the most appropriate threshold was recorded in each case, based on the minimum distance criterion. An overall threshold was then selected, based on an overall assessment of the derived thresholds at the different time points. The analysis was performed in R based on the package “tdROC”, which calculates the time-dependent sensitivity, specificity and area under the curve using a nonparametric weighting adjustment.[5] Furthermore, a bootstrapping procedure was applied to validate the stability of the detected threshold. Particularly, 10000 bootstrap samples, which were equal in size to the originally selected population, were randomly generated with replacement from the originally selected CLL population. Subsequently, for each bootstrap sample, the same procedure based on the time-dependent ROC analysis was applied. The derived thresholds in each case were recorded

resulting in the threshold distribution for each time point. This enabled us to evaluate/validate the thresholds detected in the originally selected CLL population. The percentages observed for the original thresholds were both for the TTFT and the OS the prevalent percentages with markedly difference from all the other thresholds considered, thus signifying their predominance and validating the original selection. Finally, the Harrell's concordance index was calculated for each multivariable Cox model to assess the discriminatory ability of the Cox model.[6]

SUPPLEMENTARY FIGURES

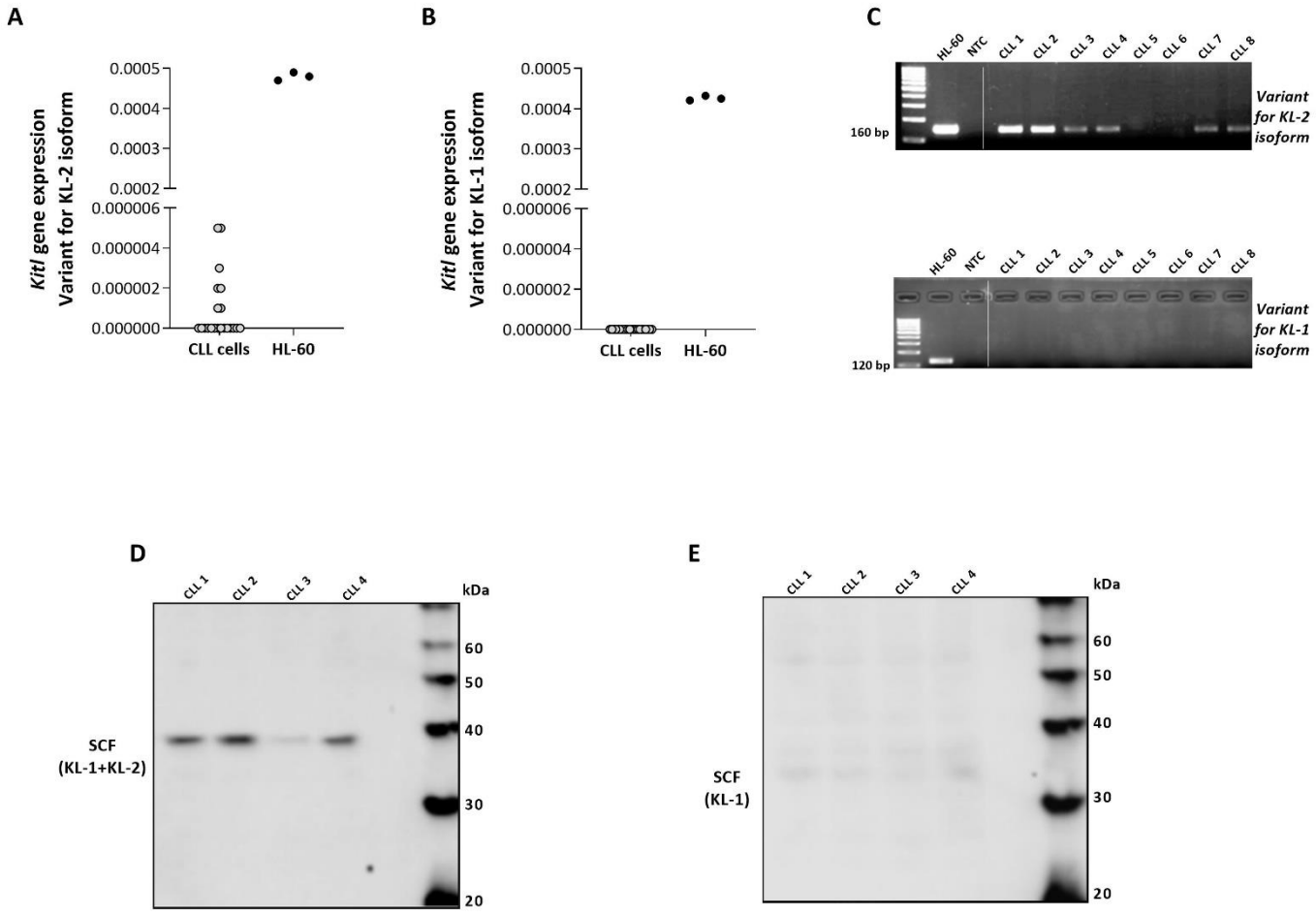

Supplementary Figure 1: (A-C) RQ-PCR analysis for the expression of the *KITLG* gene splice variants in CLL cells. The promyelocytic leukemia cell line HL-60 was used as a positive control. In (C), representative agarose gel with the products of the RQ-PCR experiments. **(D)** Representative Western Blot of the protein expression of total SCF protein levels (KL-1+KL-2 isoforms, 37 kDa) in CLL cells. **(E)** Representative Western Blot of the SCF isoform KL-1 in CLL cells (32 kDa).

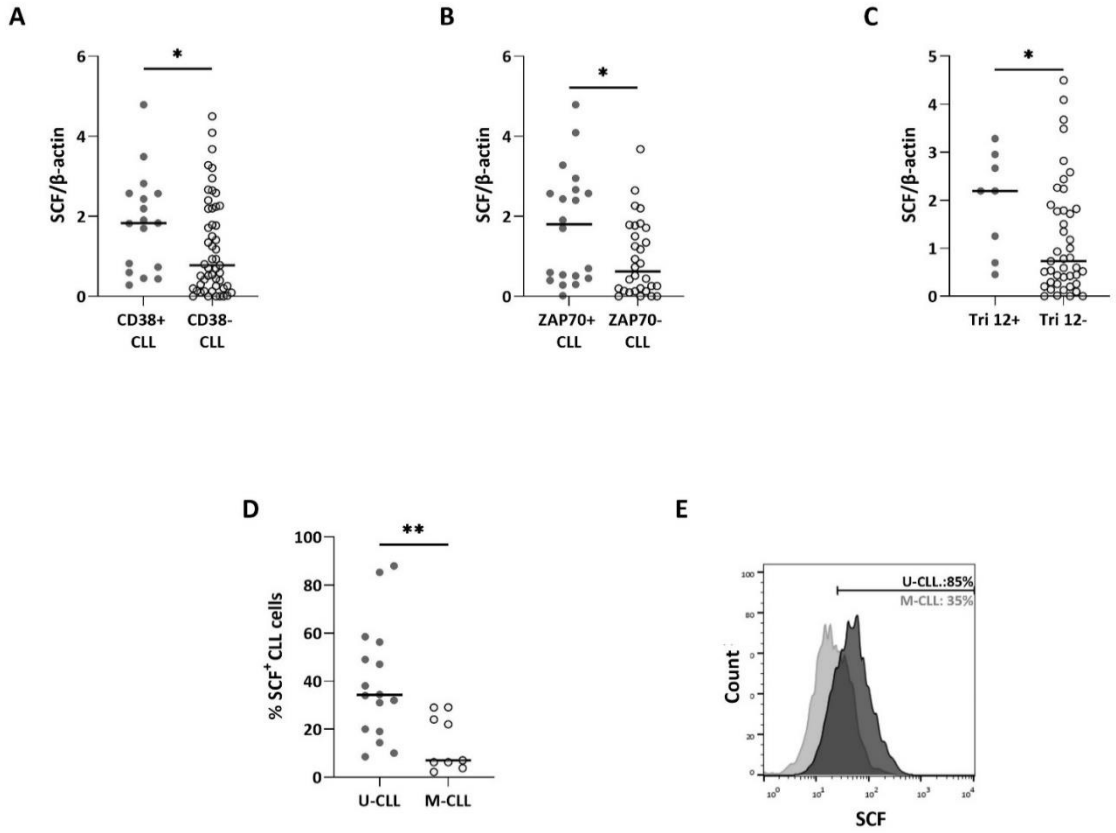

Supplementary Figure 2: **(A-C)** SCF is overexpressed in CD38$^+$, ZAP70$^+$ and Trisomy 12$^+$ (Tri12$^+$) CLL cases. The dot plot shows normalized SCF protein levels to β-actin from Western Blot studies and each dot represents one case. **(D)** Comparison of SCF positive cells (flow cytometry for viable/SCF$^+$ CLL cells) from U-CLL and M-CLL cases. **(E)** Representative histogram from Flow Cytometry analysis depicting SCF+ cells in one U-CLL and one M-CLL case. The significant difference was analyzed by the Mann–Whitney U test; *p<0.05, ***p<0.001.

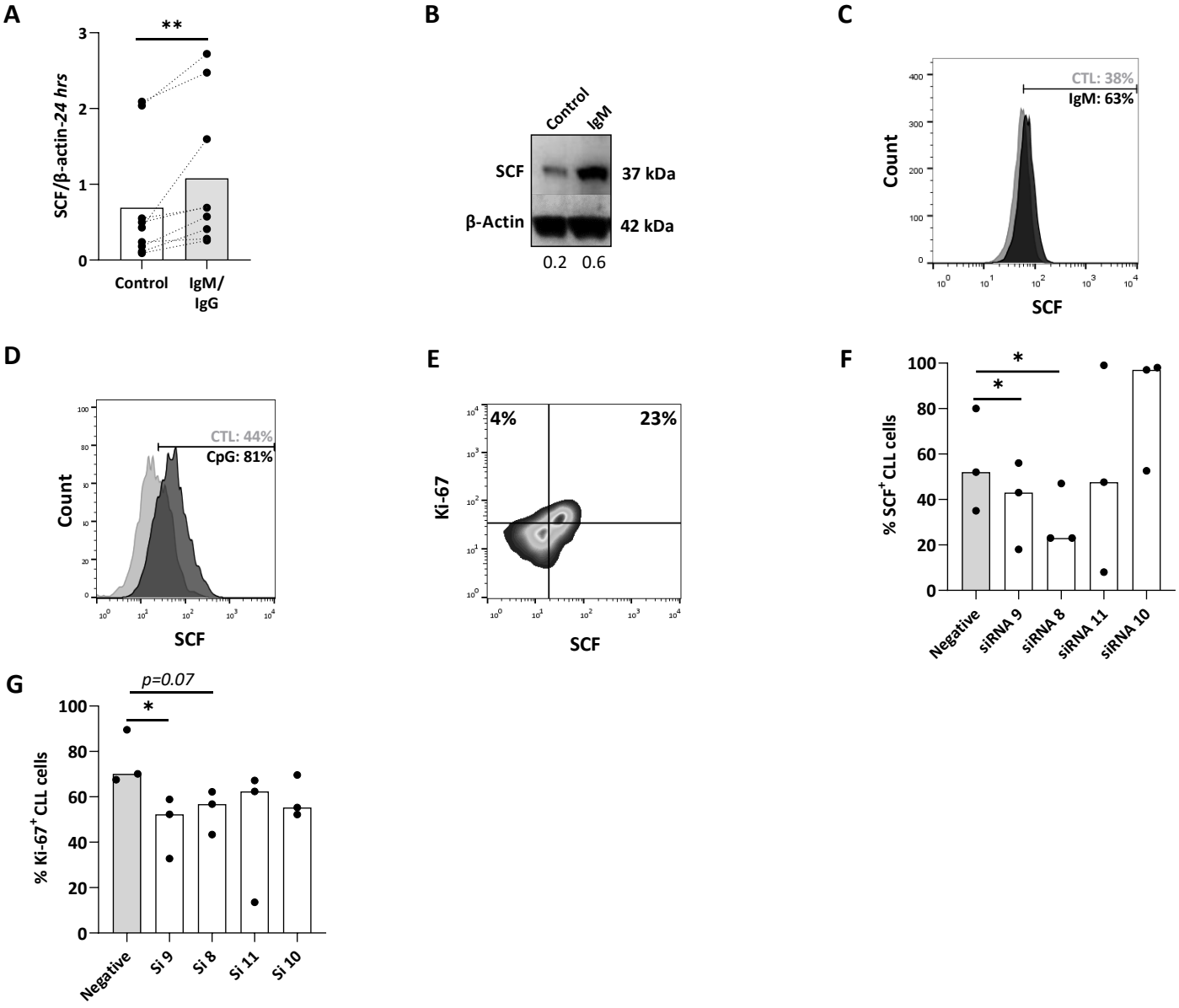

Supplementary Figure 3: (**A**) Comparison of SCF protein expression (Western blot analysis) from untreated (Control) and Ig-stimulated U-CLL cells; SCF protein levels were normalized to β-actin. (**B**) Representative Western blot for SCF protein levels in a single CLL case for untreated (Control) and stimulated U-CLL cells. (**C**) Representative histogram from flow cytometry analysis for SCF+ cells in untreated (Control) and IgM-stimulated U-CLL cells. (**D**) Representative histogram from flow cytometry analysis for SCF+ cells in untreated (Control) and CpG-stimulated U-CLL cells. (**E**) Representative dot plot from flow cytometry analysis showing proliferating (Ki-67$^+$) and SCF$^+$ CLL cells. Interconnected dots represent one case in two different conditions while bars represent median values. The Wilcoxon P test was applied to evaluate statistical significance; *p<0.05, **p<0.01, ***p<0.001. FD: Fold Difference

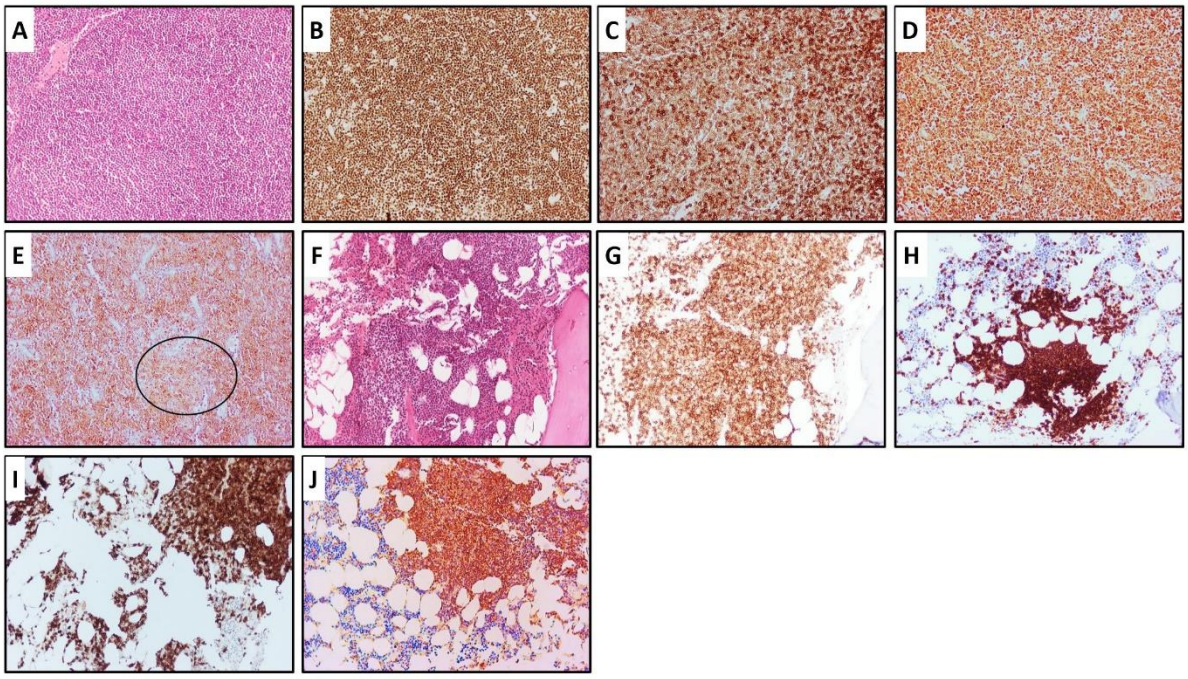

Supplementary Figure 4: **(A-E)** A case of lymph node infiltrated by CLL cells (A), being positive for PAX5 (B), CD5 (C), CD23 (D) and SCF (E). The black circle designates a proliferation center of CLL cells in the lymph node microenvironment. (**F-J**) A case of bone marrow infiltration by CLL cells. The neoplastic lymphoid cells are of small size and monomorphic (F) presenting positivity to CD20 (G), CD5 (H), CD23 (I) and SCF (J). (A,F: HEX200; B-F IHC X200).

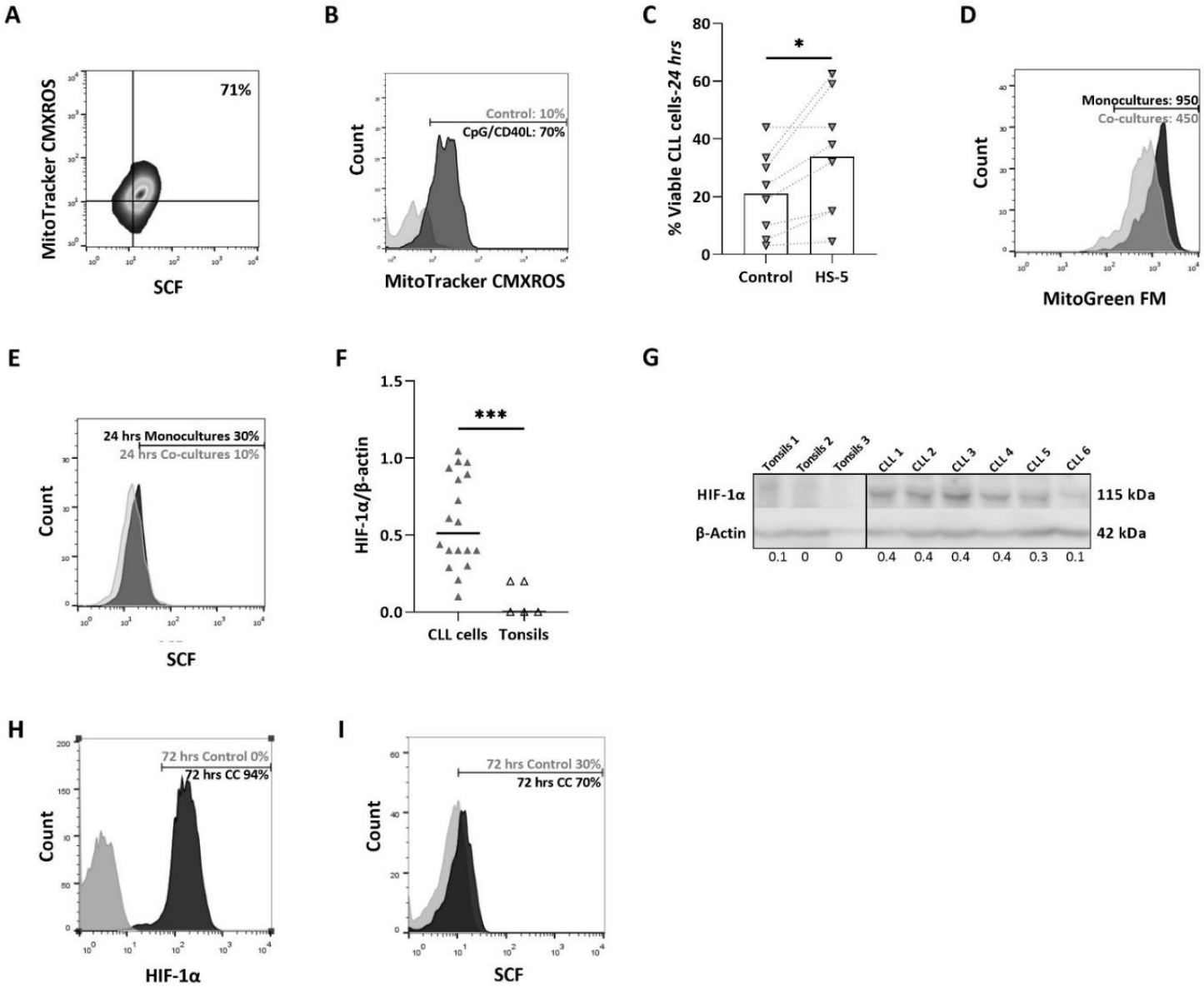

Supplemental Figure 5: (A) Representative dot plot from flow cytometry analysis showing CpG-stimulated CLL cells with active membrane potential and SCF positivity (**B**) Representative histograms from flow cytometry experiments showing the membrane potential of untreated (controls) and CpG/CD40L-stimulated cells for 1 CLL case (**C**) Viability of CLL cells co-cultured with the mesenchymal HS-5 cells for 24 hours: flow cytometry analysis of Annexin$^-$/PI$^-$ CLL cells. Interconnected dots represent one case in two different conditions while bars represent median values. (**D**) Representative histogram from flow cytometry analysis showing the mitochondrial mass of monocultured (black) and co-cultured CLL cells with the mesenchymal HS-5 cells (grey) for 24 hours. (**E**) Representative histogram from flow cytometry analysis

showing SCF positivity in monocultured (black) and co-cultured CLL cells with the mesenchymal HS-5 cells (grey) for 24 hours. (**F**) Comparison of HIF-1α protein expression in CLL cells versus healthy tonsillar B cells. The dot plot shows HIF-1α protein levels normalized to β-actin from Western blot studies and each dot represents one case. (**G**) Representative Western Blot for the distinct HIF-1α probing in samples from healthy tonsils and CLL cases. (**H-I**) Representative histograms from flow cytometry analysis showing HIF-1α and SCF positivity respectively in monocultured (grey) and co-cultured CLL cells with the mesenchymal HS-5 cells (grey) for 72 hours. Interconnected dots represent one case in two different conditions while bars represent median values. The Wilcoxon P test was applied to evaluate statistical significance; *p<0.05, **p<0.01, ***p<0.001 in 5C. The significant difference was analyzed by the Mann–Whitney U test; *p<0.05, ***p<0.001 in 5F FD: Fold Difference

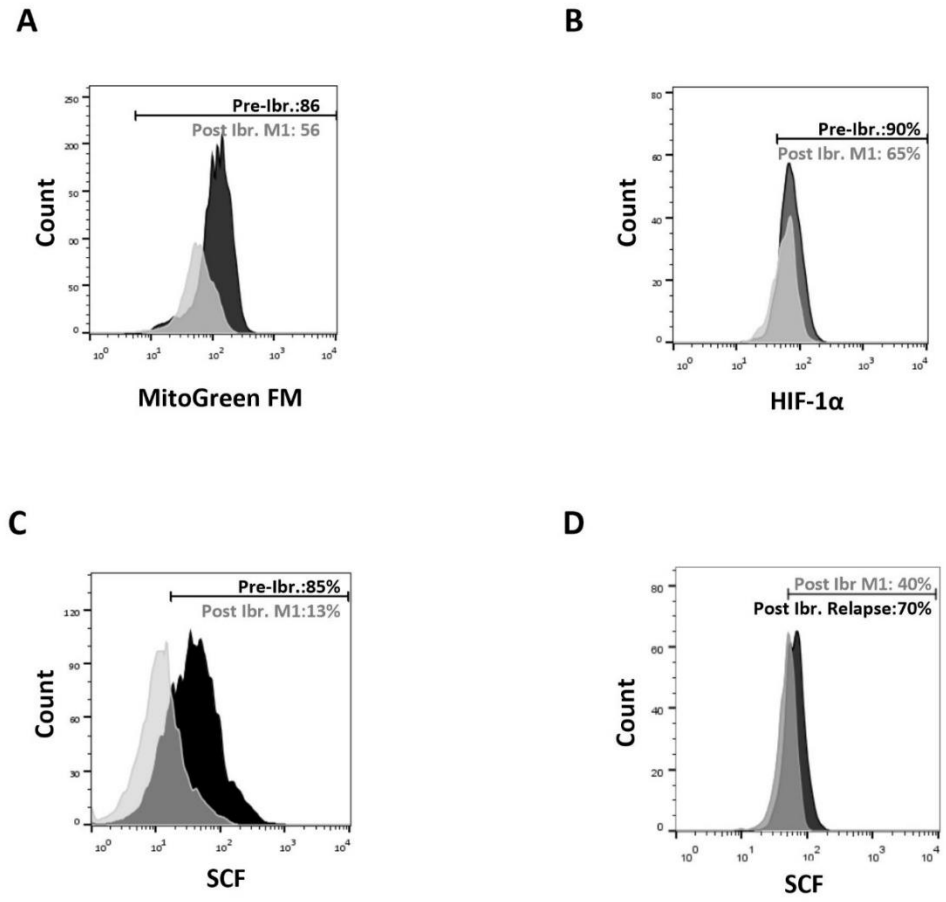

Supplemental Figure 6: (A-C) Representative histograms from flow cytometry analysis of mitochondrial mass (A), HIF-1a positivity (B) and SCF positivity (C) in CLL samples before (black) and 1 month under Ibrutinib therapy (grey). (**D**) Representative histogram from flow cytometry analysis of SCF positivity in CLL samples 1 month under Ibrutinib therapy and at the point of relapse (black).

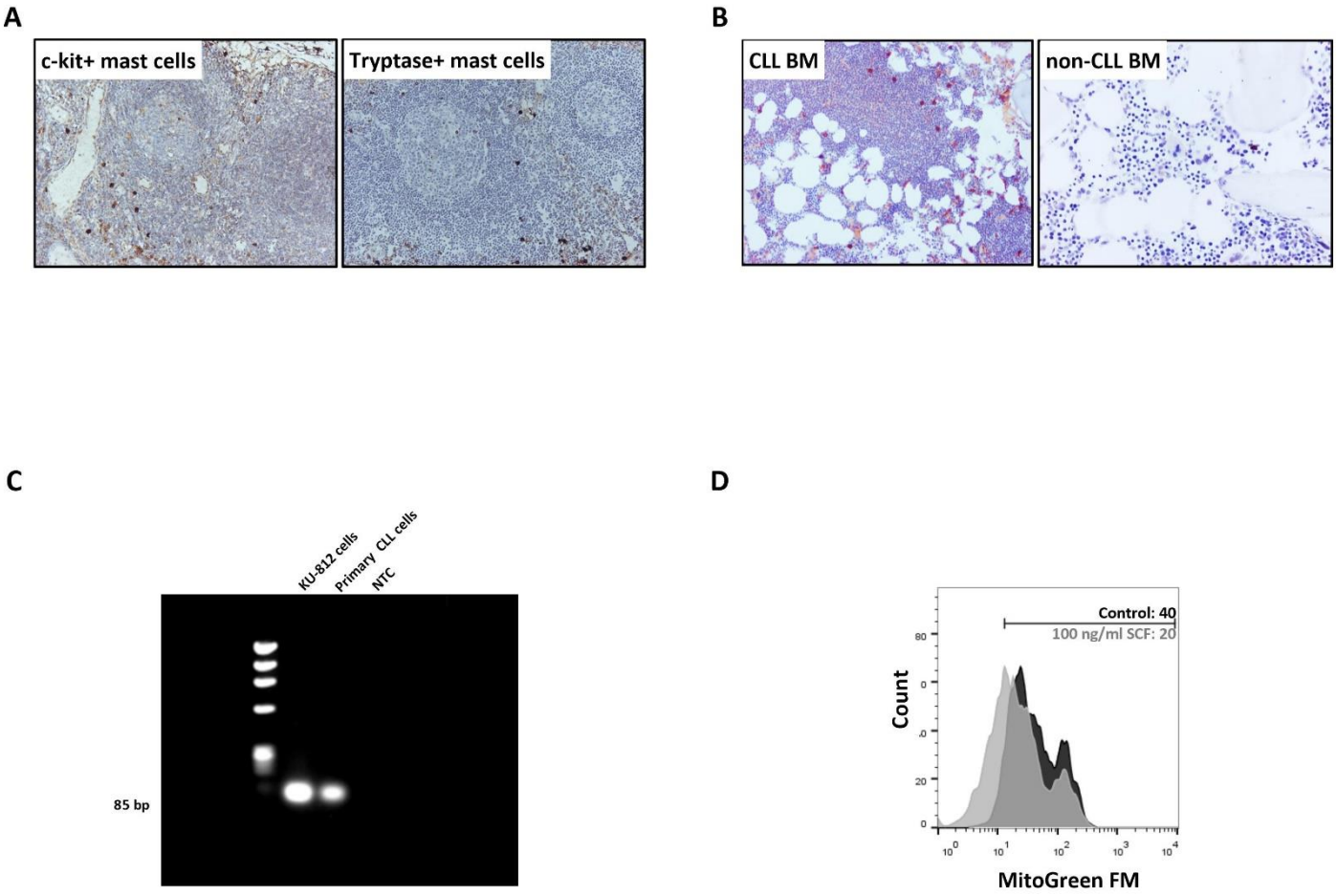

Supplemental Figure 7: (A) Lymph nodes presenting scattered c-Kit positive cells proven to be mast cells in tryptase immunostain. (**B**) Infiltrating c-Kit positive mast cells in a CLL bone marrow and in reactive, non-CLL bone marrow (IHC X200). **(C)** Representative agarose electrophoresis of the RQ-PCR products regarding the expression of the *KIT* gene in CLL cells. KU-812 chronic myelogenous leukemia cell line was used as a positive control. (**D**) Representative histogram from flow cytometry analysis depicting the mitochondrial mass of untreated CLL cells (black) or treated with 100 ng/ml SCF (grey) for 48 hours.

SUPPLEMENTARY TABLES

Supplementary Table 1. Demographic, clinical and biological data for studies associating SCF protein expression to risk factors

Patient id	Age at diagnosis	Sex	Rai at diagnosis	Binet at diagnosis	Surface IGH isotype	Surface CD38	Intracellular ZAP-70	Karyotype	FISH trisomy 12	Progression	OS (Months)	TTFT (Months)	Mutational status of IGHV genes
P10029	57	F	I	A	MD	POSITIVE	POSITIVE	46,X,-X,+12[13]/46,XX[7]	POSITIVE	PROGRESSIVE	139	83	UNMUTATED
P10343	70	F	0	A	D	NEGATIVE	NEGATIVE	46,XX[25]	NEGATIVE	STABLE	72	72	MUTATED
P10393	55	M	0	A	MD	NEGATIVE	NEGATIVE	46,XY[20]	NEGATIVE	STABLE	87	87	MUTATED
P1050	65	F	n/a	n/a	G	POSITIVE	N/A	46,XX,t(9;13)(p21;q14),del(17)(p13)[6]/46,XX[10]	NEGATIVE	PROGRESSIVE	70	4	UNMUTATED
P10635	57	M	I	A	MD	NEGATIVE	NEGATIVE	46,XY,idic(21)(p11)[3]/45,sl,der(14)t(6;14)(p11;p11),-15[15]/45,sld,del(11)(q23)[2]/46,XY[6]	NEGATIVE	STABLE	74	74	UNMUTATED
P10650	64	M	I	A	MD	NEGATIVE	NEGATIVE	46,XY[20]	NEGATIVE	PROGRESSIVE	35	14	UNMUTATED
P10722	69	M	0	A	N/A	NEGATIVE	NEGATIVE	46,XY,9q+[28]	NEGATIVE	STABLE	77	77	MUTATED
P11330	59	F	I	A	MD	NEGATIVE	NEGATIVE	46,XX[20]	NEGATIVE	STABLE	77	77	MUTATED

Patient id	Age at diagnosis	Sex	Rai at diagnosis	Binet at diagnosis	Surface IGH isotype	Surface CD38	Intracellular ZAP-70	Karyotype	FISH trisomy 12	Progression	OS (Months)	TTFT (Months)	Mutational status of IGHV genes
P1156	64	F	II	A	M	POSITIVE	POSITIVE	47,XX,inv(9)(p13q22),+12[3]/47,XX,t(1;13)(p12;q12),inv(9)(p13q22)+12[3]/46,XX[24]		PROGRESSIVE	167	113	MUTATED
P1173	63	F	I	A	MD	NEGATIVE	POSITIVE	46,XX[20]	POSITIVE	PROGRESSIVE	166	14	UNMUTATED
P11778	51	M	0	A	MD	NEGATIVE	NEGATIVE	46,XY[20]	NEGATIVE	STABLE	52	52	MUTATED
P1188	59	M	II	B	MD	NEGATIVE	NEGATIVE	46,XY[20]	NEGATIVE	STABLE	168	168	MUTATED
P12206	66	M	I	A	MD	NEGATIVE	N/A	N/A	N/A	PROGRESSIVE	64	56	UNMUTATED
P12261	67	M	0	A	MD	NEGATIVE	NEGATIVE	46,XY[20]	NEGATIVE	STABLE	59	59	MUTATED
P12452	56	F	I	A	MD	NEGATIVE	NEGATIVE	N/A	NEGATIVE	PROGRESSIVE	81	62	MUTATED
P1615	62	F	0	A	G	NEGATIVE	POSITIVE	47,XX,+12[28]/47,sl,del(6)(q31q35)[1]/46,XX[14]	POSITIVE	PROGRESSIVE	185	93	UNMUTATED
P18780	61	F	0	A	M	NEGATIVE	POSITIVE	46,XX[20]	NEGATIVE	PROGRESSIVE	70	35	UNMUTATED
P1894	53	M	0	A	M	NEGATIVE	N/A	46,XY[20]	NEGATIVE	STABLE	161	1	MUTATED
P21610	47	M	I	A		N/A	N/A	46,XY[47]	NEGATIVE	PROGRESSIVE	162	29	UNMUTATED
P21735	62	F	II	B	MD	NEGATIVE	N/A	46,XX,t(14;22)(q34;q11)[6]/46XX[22]	NEGATIVE	PROGRESSIVE	14	13	UNMUTATED
P22054	74	F	0	A	MD	NEGATIVE	N/A	46,XX,del(11)(q23q24)[8]/46,XX[12]	NEGATIVE	STABLE	21	21	UNMUTATED

Patient id	Age at diagnosis	Sex	Rai at diagnosis	Binet at diagnosis	Surface IGH isotype	Surface CD38	Intracellular ZAP-70	Karyotype	FISH trisomy 12	Progression	OS (Months)	TTFT (Months)	Mutational status of IGHV genes
P22210	63	M	II	B	MD	NEGATIVE	N/A	46,XY, del(17)(p13)[3]/ 45, X,- Y[3]/46,XY[24]	N/A	PROGRESSIVE	26	2	UNMUTATED
P2355	54	M	II	A	MD	NEGATIVE	POSITIVE	46,XY[20]	N/A	PROGRESSIVE	71	62	UNMUTATED
P2446	73	M	0	A	G	POSITIVE	N/A	47,XY,+12[2]/46 ,XY[24]	POSITIVE	PROGRESSIVE	101	62	UNMUTATED
P2512	54	F	I	A	MD	POSITIVE	POSITIVE	43- 45,XX,add(2)(q2 ?7),t(8;17)(p2?3 ;q11),-13,-17,- 18,+mar[cp9]/4 6,XX[15]	NEGATIVE	PROGRESSIVE	247	41	UNMUTATED
P2528	52	F	I	A	f	NEGATIVE	NEGATIVE	46,XX	N/A	STABLE	146	146	MUTATED
P2548	69	M	I	A	MD	NEGATIVE	N/A	46,X,t(Y;11)(q12 ;q23),del(13)(q1 2q14)[11]/46,XY ,t(3;5)(q29;q23) [2]/46,XY[25]	N/A	PROGRESSIVE	66	16	UNMUTATED
P280	60	M	0	A	MD	NEGATIVE	N/A	46,XY,t(9;12)(q1 2;p11)[3]/46,XY[22]	N/A	STABLE	171	171	MUTATED
P3041	65	M	II	A	MD	NEGATIVE	N/A	46,XY[20]	NEGATIVE	PROGRESSIVE	141	19	UNMUTATED
P3123	80	F	I	A	MD	NEGATIVE	NEGATIVE	46,XX[20]	NEGATIVE		114	114	MUTATED
P32166	75	M	0	A	MD	NEGATIVE	N/A	46,XX[20]	NEGATIVE	STABLE	2	2	MUTATED
P3255	81	M	II	B	MD	POSITIVE	N/A	46,XY[20]	N/A	PROGRESSIVE	90	2	UNMUTATED

Patient id	Age at diagnosis	Sex	Rai at diagnosis	Binet at diagnosis	Surface IGH isotype	Surface CD38	Intracellular ZAP-70	Karyotype	FISH trisomy 12	Progression	OS (Months)	TTFT (Months)	Mutational status of IGHV genes
P3492	39	M	I	A	G	POSITIVE	N/A	46,XY[20]	NEGATIVE	PROGRESSIVE	143	34	UNMUTATED
P3551	59	F	0	A	G	NEGATIVE	N/A	46,XX[20]	NEGATIVE	STABLE	259	259	MUTATED
P3810	66	M	II	A	MD	POSITIVE	POSITIVE	46,XY,del(10)(q22q24)[9]/46,XY[16]	N/A	PROGRESSIVE	101	1	UNMUTATED
P3916	43	M	0	A	G	NEGATIVE	NEGATIVE	46,XY[20]	N/A	STABLE	131	131	MUTATED
P4438	75	F	0	A	MD	NEGATIVE	NEGATIVE	46,XX[20]	NEGATIVE	STABLE	93	13	MUTATED
P4557	58	F	0	A	MD	NEGATIVE	NEGATIVE	45,X,-X,inv(9)(p11q13)[3]/46,XX,inv(9)(p11q13)[17]	NEGATIVE	STABLE	146	146	MUTATED
P4994	68	M	0	A	M	NEGATIVE	NEGATIVE	46,XY[20]	NEGATIVE	PROGRESSIVE	121	93	MUTATED
P5063	59	M	I	A	G	NEGATIVE	NEGATIVE	46,XY[20]	POSITIVE	STABLE	156	156	UNMUTATED
P511	64	M	II	B	MD	NEGATIVE	N/A	N/A	N/A	PROGRESSIVE	95	40	UNMUTATED
P5231	57	M	II	B	MD	POSITIVE	NEGATIVE	46,XY[20]	NEGATIVE	PROGRESSIVE	93	30	UNMUTATED
P5283	61	M	I	A	MD	POSITIVE	POSITIVE	46,XY[20]	NEGATIVE	PROGRESSIVE	80	35	MUTATED
P5642	63	M	0	A	MD	NEGATIVE	NEGATIVE	46,XY,der(2)t(2;?)(p15),der(13)t(13;?)(q22 ;?)[12]/46,XY[3]	NEGATIVE	PROGRESSIVE	14	0	UNMUTATED
P571	48	M	0	A	MD	NEGATIVE	N/A	47,XY,+12[13]/46,XY[2]	POSITIVE	PROGRESSIVE	148	54	UNMUTATED
P5728	53	M	I	A	MD	POSITIVE	NEGATIVE	46,XY[20]	NEGATIVE	STABLE	115	115	MUTATED
P5744	55	M	0	A	MD	NEGATIVE	NEGATIVE	46,XY[20]	NEGATIVE	STABLE	110	110	MUTATED
P6068	76	F	0	A	MD	NEGATIVE	NEGATIVE	N/A		PROGRESSIVE	74	31	MUTATED

Patient id	Age at diagnosis	Sex	Rai at diagnosis	Binet at diagnosis	Surface IGH isotype	Surface CD38	Intracellular ZAP-70	Karyotype	FISH trisomy 12	Progression	OS (Months)	TTFT (Months)	Mutational status of IGHV genes
P6077	74	M	IV	C	MD	NEGATIVE	POSITIVE	46,XY,i(17)(q10)[1]/46,XY[29]	POSITIVE	PROGRESSIVE	55	8	UNMUTATED
P608	53	M	0	A	MD	NEGATIVE	N/A	46,XY[20]	NEGATIVE	N/A	220	220	MUTATED
P6124	69	M	0	A	MD	NEGATIVE	NEGATIVE	46,XY[20]	NEGATIVE	PROGRESSIVE	114	47	UNMUTATED
P6237	82	F	0	A	MD	NEGATIVE	POSITIVE	47,XX,+12[22]/46,XX[4]	POSITIVE	STABLE	32	32	UNMUTATED
P6856	58	M	0	A	MD	NEGATIVE	NEGATIVE	46,XY,t(2;18)(p13;q23)[15]/46,XY[6]	NEGATIVE	STABLE	106	106	MUTATED
P7155	51	M	0	A	MD	NEGATIVE	POSITIVE	46,XY[25]	NEGATIVE	PROGRESSIVE	105	82	UNMUTATED
P7317	80	M	III	C	MD	POSITIVE	POSITIVE	46,XY[20]	NEGATIVE	PROGRESSIVE	42	2	UNMUTATED
P7648	76	F	0	A	MD	NEGATIVE	POSITIVE	46, XX,del(5)(q31q33)[7]/46,XX[23]	NEGATIVE	PROGRESSIVE	39	3	UNMUTATED
P7981	66	M	I	A	MD	NEGATIVE	NEGATIVE	46,XY[20]		PROGRESSIVE	96	80	UNMUTATED
P8458	52	M	I	A	G	NEGATIVE	POSITIVE	46,XY[20]	NEGATIVE	PROGRESSIVE	106	48	MUTATED
P8655	66	M	II	B	MD	NEGATIVE	NEGATIVE	N/A	N/A	PROGRESSIVE	154	34	UNMUTATED
P8762	63	M	I	A		POSITIVE	POSITIVE	N/A	N/A	PROGRESSIVE	52	5	UNMUTATED
P8785	51	F	0	A	MD	NEGATIVE	NEGATIVE	46,XX[20]	NEGATIVE	STABLE	153	153	MUTATED
P9001	66	M	I	A	MD	NEGATIVE	NEGATIVE	46,XY[20]	NEGATIVE	PROGRESSIVE	100	66	UNMUTATED
P9208	43	M	I	A	G	POSITIVE	NEGATIVE	49,XY,+12,+18,+19[15]/46,XY[5]		STABLE	96	96	MUTATED
P9391	84	M	III	C	MD	POSITIVE	POSITIVE	46,XY[20]	NEGATIVE	PROGRESSIVE	41	0	MUTATED

Patient id	Age at diagnosis	Sex	Rai at diagnosis	Binet at diagnosis	Surface IGH isotype	Surface CD38	Intracellular ZAP-70	Karyotype	FISH trisomy 12	Progression	OS (Months)	TTFT (Months)	Mutational status of IGHV genes
P9548	68	F	I	A	MD	NEGATIVE	NEGATIVE	46,XX,del(11)(q14q23.1)[8]/46,sl,del(13(q12q14)[3]/46,XX[10]	NEGATIVE	PROGRESSIVE	88	56	UNMUTATED
P9605	71	M	0	A	G	NEGATIVE	POSITIVE	46,XY[20]	NEGATIVE	STABLE	85	85	MUTATED
P9709	53	F	II	B	MD	POSITIVE	N/A	46,XX,der(4)t(3;4)9q21;p16),t(11;14)(q13;q32)[8]/46,sl,add(18)(p11)[3]/46,XX[13]	NEGATIVE	PROGRESSIVE	96	74	UNMUTATED
P9756	72	M	I	A	MD	NEGATIVE	NEGATIVE	46,XY,del(11)(q14q23)[5]/46,sl,del(13)(q12q14)[3]/46,XY[12]	NEGATIVE	PROGRESSIVE	81	17	UNMUTATED
P8071	N/A	M	N/A	N/A	MD	POSITIVE	POSITIVE	N/A	NEGATIVE	N/A	N/A	N/A	UNMUTATED

Supplementary table 2. For the studies concerning the longitudinal expression profile of SCF protein expression in CLL cases under Ibrutinib therapy, we analyzed samples from a cohort of 10 CLL patients that were obtained: (a) prior to Ibrutinib therapy (Pre-Ibrutinib) and (b) 1 month after Ibrutinib therapy (Post-Ibrutinib).

Patient id	Age at diagnosis	Sex	Rai at diagnosis	Binet at diagnosis	Surface IGH isotype	Surface CD38	Intracellular ZAP-70	Karyotype	FISH trisomy 12	Progression	Loss of response to Ibrutinib	TTFT (Months)	Mutational status of IGHV genes
P21610	47	M	I	A		N/A	N/A	46,XY[47]	NEGATIVE	PROGRESSIVE	NO	29	UNMUTATED
P21735	62	F	II	B	MD	NEGATIVE	N/A	46,XX,t(14;22)(q34;q11)[6]/46XX[22]	NEGATIVE	PROGRESSIVE	NO	13	UNMUTATED
P1173	63	F	I	A	MD	NEGATIVE	POSITIVE	46,XX[20]	POSITIVE	PROGRESSIVE	YES	14	UNMUTATED
P18780	61	F	0	A	M	NEGATIVE	POSITIVE	46,XX[20]	NEGATIVE	PROGRESSIVE	NO	35	UNMUTATED
P12336	60	M	II	A	MD	NEGATIVE	NEGATIVE	N/A	NEGATIVE	PROGRESSIVE	NO	0	UNMUTATED
P11323	67	M	0	A	MD	NEGATIVE	NEGATIVE	46,XY[20]	NEGATIVE	PROGRESSIVE	NO	2	UNMUTATED
P9320	47	M	I	A	MD	POSITIVE	POSITIVE	46,XY[20]	NEGATIVE	PROGRESSIVE	NO	5	UNMUTATED
P7647	55	M	II	B	MD	POSITIVE	POSITIVE	46,XY,-17,+mar[5]/ 46,XY[20]	NEGATIVE	PROGRESSIVE	NO	0	UNMUTATED
P30572	0	M	N/A	N/A	N/A	N/A	N/A	N/A	N/A	N/A	NO	0	UNMUTATED
P21499	61	M	I	A	N/A	N/A	N/A	N/A	NEGATIVE	N/A	NO	0	UNMUTATED
P8755	69	M	II	B	M	NEGATIVE	POSITIVE	46,XY[20]	NEGATIVE	PROGRESSIVE	YES	0	UNMUTATED
P22210	62	M	II	B	MD	NEGATIVE	N/A	46,XY, del(17)(p13)[3]/ 45, X,-Y[3]/46,XY[24]	N/A	PROGRESSIVE	YES	2	UNMUTATED
P4656	51		0	A	MD	NEGATIVE	N/A	46,XY[20]	N/A	PROGRESSIVE	YES	20	UNMUTATED

Supplementary Table 3: List of the antibodies used for western blotting and flow cytometry experiments. WB: western blotting, FCM: Flow cytometry, IHC: Immunohistochemistry

Antibody used	Catalogue Number	Company	Application
Recombinant Anti-SCF antibody [EP665Y]	ab52603	Abcam	WB, FCM,IHC
Anti-SCF antibody	ab83866	Abcam	WB
Human/Mouse/Rat HIF-1 alpha Antibody	MAB1536	R&D Systems	WB, FCM
Rabbit polycolonal c-Kit (CD117) antibody	A4502	Dako	IHC
Recombinant Rabbit IgG, monoclonal [EPR25A] - Isotype Control	ab172730	Abcam	FCM
Goat anti-Mouse IgG (H+L) Secondary Antibody, FITC	A16067	ThermoFischer Scientific	FCM
Goat Anti-Rabbit IgG H&L (Phycoerythrin) preadsorbed	ab72465	Abcam	FCM
Goat Anti-Rabbit IgG H&L (HRP)	ab97051	Abcam	WB
FITC Mouse Anti-Ki-67 Set	556026	BD	FCM
PE-Cy™5 Mouse Anti-Human CD19, Clone HIB19	555414	BD	FCM
Goat anti-Rabbit IgG (H+L) Secondary Antibody, FITC	65-6111	ThermoFischer Scientific	FCM

Supplementary Table 4: Survival analysis for the correlation of SCF protein expression with Overall Survival (OS) and Time-To-First Treatment (TTFT) in CLL cases. SCF protein expression are SCF protein levels normalized to β-actin from Western Blot studies. ***p<0.001.

	SCF high/low CLL patients	Number of CLL patients	Median (Months)	logrank	Hazard ratio	C-index
OS	SCF^{high} patients > 1.7	42	101	p=0.0003	4.496 (1.829-11.05)	0.676
	SCF^{low} patients ≤ 1.7	26	185		p=0.00105	
TTFT	SCF^{high} patients > 0.93	34	35	p=0.0008	3.24 (1.66-6.31)	0.647
	SCF^{low} patients ≤ 0.93	34	113		p= 0.00055	

REFERENCES

1. Arvaniti E, Ntoufa S, Papakonstantinou N, et al. Toll-like receptor signaling pathway in chronic lymphocytic leukemia: Distinct gene expression profiles of potential pathogenic significance in specific subsets of patients. Haematologica 2011;96(11):1644–1652.
2. Valceckiene V, Kontenyte R, Jakubauskas A, Griskevicius L. Selection of reference genes for quantitative polymerase chain reaction studies in purified B cells from B cell chronic lymphocytic leukaemia patients. Br J Haematol 2010;151(3):232–238.
3. Livak KJ, Schmittgen TD. Analysis of Relative Gene Expression Data Using Real-Time Quantitative PCR and the 2−ΔΔCT Method. Methods 2001;25(4):402–408.
4. Heagerty PJ, Lumley T, Pepe MS. Time-dependent ROC curves for censored survival data and a diagnostic marker. Biometrics 2000;56(2):337–344.
5. Li L, Greene T, Hu B. A simple method to estimate the time-dependent receiver operating characteristic curve and the area under the curve with right censored data. Stat Methods Med Res 2018;27(8):2264–2278.
6. Harrell FE, Califf RM, Pryor DB, Lee KL, Rosati RA. Evaluating the Yield of Medical Tests. JAMA J Am Med Assoc 1982;247(18):2543–2546.